

# Relaxations of Bisphenol A-Based Epoxides Cured with Aliphatic Diamines

MAMI MATSUKAWA,<sup>1,\*</sup> HIROTAKE OKABE,<sup>2</sup> and KAZUMI MATSUSHIGE<sup>3</sup>

<sup>1</sup>Material Physics Department, Government Industrial Research Institute, Osaka, Midorigaoka, Ikeda, Osaka 563, Japan; <sup>2</sup>Department of Applied Science, Faculty of Engineering, Kyushu University, 36 Higashi-ku, Fukuoka 812, Japan; <sup>3</sup>Department of Electronics, Faculty of Engineering, Kyoto University, Sakyo-ku, Kyoto 606, Japan

## SYNOPSIS

The main  $\alpha$  and sub  $\beta$  relaxations in bisphenol A-based epoxides cured by two kinds of aliphatic diamines were examined in wide temperature and frequency ranges by using middle-frequency dynamic, dielectric, and ultrasonic measuring systems. The obtained temperature–frequency correlation maps revealed an Arrhenius-type behavior for the  $\beta$  relaxation with apparent activation energy of 16 kcal/mol. For the  $\alpha$  relaxation, the maps were in good agreement with the W.L.F. equation. Owing to the similarity of structure in these resins, both maps showed the same tendencies. © 1993 John Wiley & Sons, Inc.

## INTRODUCTION

Epoxides have become one of the most useful thermosetting resins in commercial use, owing to their outstanding characteristics and ease of treating. Moreover, it is well known that these polymeric materials exhibit relatively high temperature stability.

In cured epoxides, generally, three-dimensional molecular network structures are formed by crosslinking. The bonding condition of the crosslinks therefore changes depending upon the prepolymers and curing agents used, and the advance of crosslinking in resins then has a strong influence on the elasticity. This binding is also directly connected to the glass transition temperature ( $T_g$ ) and the heat-resistant ability.

At lower temperatures than  $T_g$ , the micro-Brownian motions in resins are considered to be frozen. In imperfectly cured resins, some studies have also pointed out before that the advance of crosslinking always shifts  $T_g$  to higher temperatures.<sup>1–3</sup> Moreover, this shift of  $T_g$  implies the temperature shift of the main  $\alpha$  relaxations, due to the glass transition region being closely related to the relaxation. From this point of view,  $T_g$  is often con-

sidered as the lower limit of the  $\alpha$  peak temperature at very low frequencies.<sup>4</sup> In addition, it has been pointed out that the crosslinking also affects the strength of sub  $\beta$  relaxation.<sup>5</sup> This relaxation results from a particular mode of motion within the side groups and has been called the  $\beta$  or  $\gamma$  relaxation.<sup>6</sup>

Following the studies of Ochi et al. on glassy-state epoxides,<sup>7</sup> this is regarded as the  $\beta$  relaxation for this study. Of additional interest here is the contribution of this  $\beta$  relaxation to the impact strength,<sup>7</sup> which can also be seen in thermoplastics. Therefore, the relaxation processes in epoxides have been extensively investigated during the curing process, commonly using dynamic, thermal, and dielectric measurements. Only a few studies, however, have employed the frequency–temperature correlation of these relaxations in epoxides to obtain the apparent activation energies.<sup>8</sup>

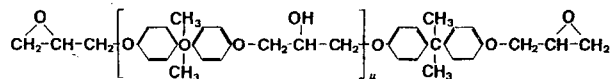
To investigate these phenomena, we have chosen to observe the frequency–temperature correlation of the main  $\alpha$  and sub  $\beta$  relaxation in bisphenol A-based epoxides. Relaxations were investigated at different frequencies and temperatures, using middle-frequency dynamic and dielectric measurements. Moreover, in the ultrasonic frequency range, the ultrasonic spectroscopy technique<sup>9,10</sup> was applied to obtain minute information of the ultrasonic properties, such as wave velocity and attenuation in the wide temperature range.

\* To whom correspondence should be addressed.

## EXPERIMENTAL

### Materials

The epoxy prepolymer used here is the diglycidyl ether of bisphenol A, commercialized under the brand name Epikote 828 (Shell). The structural formula is as follows;



It was cured with aliphatic curing agents with the structural formula



Two agents used in this study were hexamethylenediamine (HMDA,  $n = 6$ ) and octamethylenediamine (OMDA,  $n = 8$ ), in which the number of methyl groups  $n$  contained are different. Networks in resins are formed by the condensation of the prepolymer with each curing agent.

The procedure for preparing the samples is given below: the amount of each curing agent used was in the stoichiometric amounts to the prepolymer. At first, the condensation of the prepolymer and curing agent was held in vacuum for degassing to eliminate void formation. It was then cured overnight between 0 and 5°C for gelation. For heat curing, it was held for 1 h at 60°C, 3 h at 100°C, and, then, 3 h at 150°C, which has been recommended to obtain fully cured resins. After completion of curing, the resins were cooled for 12 h to room temperature, taking account of aging during this process. The resins, cured in this way, are known to be composed of highly crosslinked networks.<sup>1</sup> Moreover, the crosslinking processes in these samples are known to be the same, owing to the homology of the aliphatic curing agents used. The averaged distance between crosslinks, however, is expected to be different on account of the length of curing agents used. In these sample resins, the glass transition temperature ( $T_g$ ) then must directly reflect the condition of these networks. For this purpose,  $T_g$  was measured using a differential scanning calorimeter (DSC) built by Rigaku. All the following experiments used specimens of various shapes cut down from the same block of resins.

### Middle-frequency Dynamic Measurements

The temperature evolution of the complex dynamic Young's modulus was measured by a dynamic vis-

coelastometer (Vibron) built by Orientec. The Vibron measures the stress response of strip-shaped resins, by applying a sinusoidal tensile strain in the middle-frequency range (3.5–110 Hz). The measured temperature range was programmed from -150 to 250°C with 1°C/min heating.

### Dielectric Measurements

The dielectric loss was measured using a high-temperature cell by HP4194A impedance gain phase analyzer interfaced with a personal computer. The measurements were performed at an isothermal condition by sweeping the measuring frequencies from 50 kHz to 5 MHz and the observed temperature range was from room temperature up to 170°C.

### Ultrasonic Measurements

A pulse spectroscopy technique was employed for measuring ultrasonic properties in resins. In this technique, the use of broadband ultrasonic pulses brings detailed information over different frequencies by one measurement. Moreover, this procedure is much simpler than the continuous wave technique.

The experimental setup is given in Figure 1. Here, polyvinylidene fluoride (PVDF) piezoelectric polymer films were used as ultrasonic transducers. The sample resin and films were then connected to each other by polyimide buffers. The polyimide buffer was cut on the side wall to eliminate the surface wave

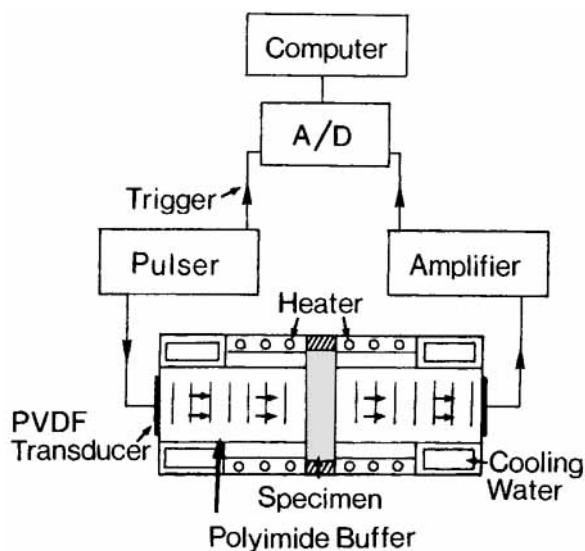


**Figure 1** Schematic diagram for ultrasonic measuring system and cell.

and reflections. The temperature of samples was controlled from room temperature to 220°C at a heating rate of 2°C/min. The films and buffers were also water-cooled to avoid the heat effect on PVDF films. During measurements, ultrasonic pulses in the MHz range are sent from one piezoelectric film to the other. The received pulses were digitized and analyzed in the frequency domain using fast Fourier transform (FFT). The amplitude spectrum then reflects directly the longitudinal attenuation, and the phase spectrum can be translated to a longitudinal wave velocity, owing to the following equation<sup>11</sup>;

$$v(\omega) = \frac{\omega L}{\phi(\omega)} \quad (1)$$

Here,  $\omega$ ,  $\phi$ , and  $L$  indicate the angular frequency, phase, and specimen thickness, respectively. In these measurements, of course, the temperature effect of polyimide buffers were also considered and eliminated in the calculation.

## RESULTS AND DISCUSSION

In this study, the  $T_g$  values were first evaluated by DSC. The  $T_g$  values are then associated with the midpoint of the jump of heat capacity in DSC experiments. As listed in Table I, both of the sample resins used showed comparatively high  $T_g$  values, which were found to be inversely proportional to the number of methyl groups present.

Figure 2 shows typical plots of the dynamic Young's modulus measured at 11 Hz for the sample resin cured with OMDA. In general, the real part  $E'$  (dynamic storage modulus) decreases dramatically as the temperature increases, whereas the imaginary part  $E''$  (dynamic loss modulus) shows two peaks,  $\alpha$  and  $\beta$ . These results indicate the existence of relaxations at this temperature and frequency, which result from the different kinetic processes in resins. The  $\alpha$  peak, which can be observed at temperatures a little higher than the  $T_g$ , has been regarded as the

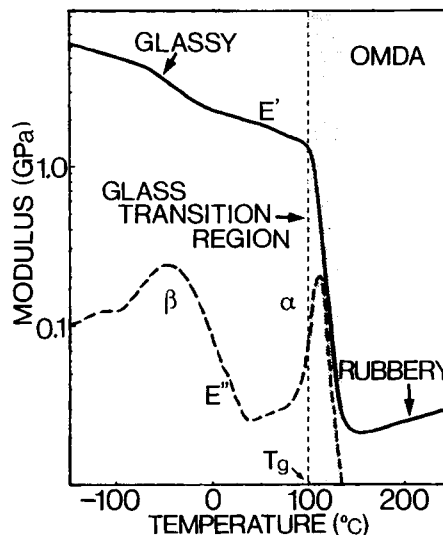


**Figure 2** Dynamic tensile modulus of cured resin measured at 11 Hz.

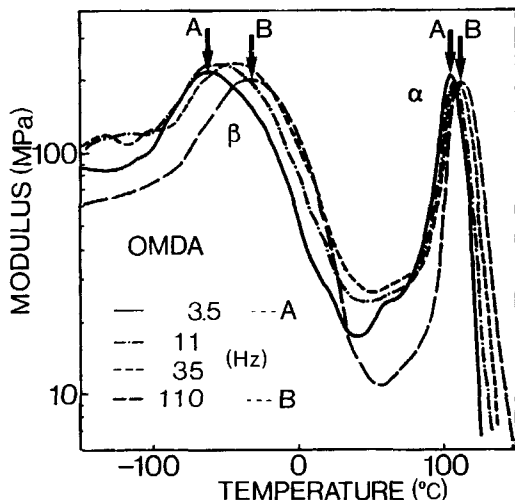
main relaxation peak. The peak temperature shifts due to the amount of crosslinks and reflects the improvement of high temperature stability.<sup>12</sup> In addition,  $E''$  varies slowly over a wide temperature range near the  $\beta$  peak. This peak is due to the sub  $\beta$  relaxation, which has been reported to result from a particular mode of motion within the side groups, which includes crosslinking.<sup>7</sup> Although the sample resins are expected to be cured perfectly,  $E'$  increased as the temperature increased over the rubbery state. One reason for this is supposed to be the effect of charring.

Figure 3 shows the temperature variation of the dynamic loss modulus  $E''$  measured at different frequencies for the resin cured with OMDA, revealing  $\alpha$  and  $\beta$  relaxation peaks. The  $\beta$  relaxation peak shifts more quickly than the  $\alpha$  relaxation peak, reflecting, probably, the difference of the activation energies. Generally, the frequency-temperature correlation of these relaxation peaks changes owing to each apparent activation energy and relaxation process. In case of thermoplastics, the  $\alpha$  relaxation processes are usually expressed by the W.L.F. expression, whereas the  $\beta$  relaxations are regarded as Arrhenius type with an apparent activation energy of 10–20 kcal/mol. In addition, the apparent activation energy of the  $\alpha$  relaxation process is generally larger than that of  $\beta$  relaxation process.<sup>12</sup> This implies that the frequency effect on the  $\alpha$  relaxation peak temperatures, compared with that of  $\beta$  relaxation, is small.

Of additional interest from dynamic measurements is the behavior of dynamic loss modulus  $E''$

**Table I** The Glass Transition Temperature ( $T_g$ ) of Resins, Measured by DSC

Curing Agent	Methyl Groups	$T_g$ (°C)
HMDA	6	100
OMDA	8	95



**Figure 3** Temperature variation of dynamic loss modulus at different frequencies.

in the glassy state. The  $\beta$  peak in this sample is comparatively strong. This phenomenon has been reported in other epoxy systems cured with diamines.<sup>13</sup> In addition, the slow changes of  $E''$  near the  $\beta$  peak possibly indicates the distribution of  $\beta$  relaxation times. In other glassy-state polymers, some sub- $T_g$  relaxations have been reported to have a distribution of relaxation times. Moreover, in epoxy resins cured with other diamines, Ochi et al. pointed out the overlapping phenomena of two different sub- $T_g$  relaxations, which consist of motion in different parts of the crosslinks.<sup>13</sup> Thus, the broad  $\beta$  peak observed for the sample resins cured with OMDA possibly suggests that several molecular motions are involved in this sub- $T_g$  relaxation phenomenon.

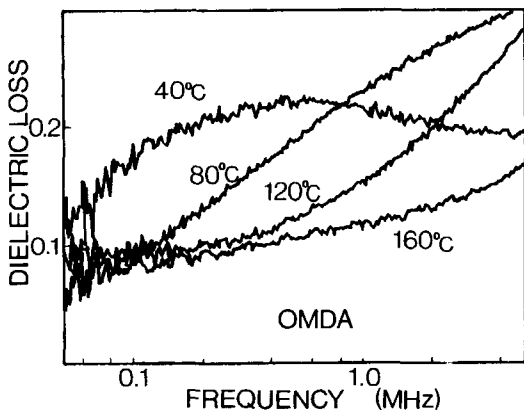


**Figure 4** Frequency dependence of dielectric loss at different temperatures.

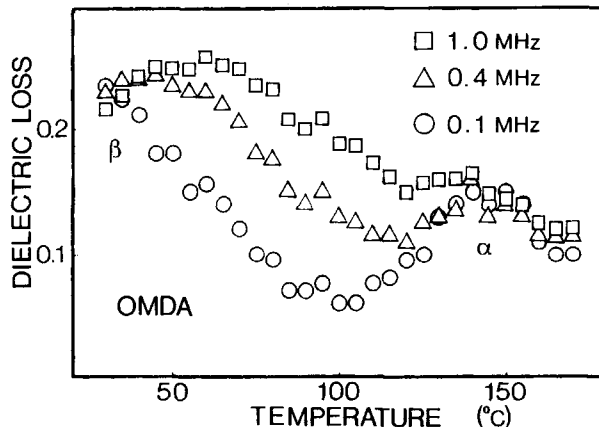


**Figure 5** Temperature dependence of dielectric loss at different frequencies.

To extract further information on the main  $\alpha$  and sub  $\beta$  relaxations, the dielectric loss in resins were measured. This is because relaxations in epoxides are derived mostly from motions of molecular sites with the dipole moment, e.g., the hydroxy-ether part in crosslinks or other side groups.<sup>14</sup> Of course, in addition to this dipole orientation, the dielectric loss composes the ionic conduction, which is considered to be inversely proportional to the frequency.<sup>15</sup> The ionic conduction effect, however, seems small in the frequencies higher than 10 kHz, as Koike has pointed out the frequency dependence of dielectric loss in an epoxy prepolymer.<sup>16</sup> Figure 4 shows the frequency dependencies of dielectric loss observed at several different temperatures. The broad dielectric loss peak seen from the datum at 40°C seems to result from the  $\beta$  relaxation. The peak position seems to move toward higher-frequency regions with increasing temperatures. The wide frequency of the broad peak also possibly implies a distribution of relaxation times. However, it seems difficult to investigate the distribution precisely because of the observed small frequency variation.

For the  $\alpha$  relaxation, it is difficult to locate the peak from the frequency dependence data. This is because the  $\alpha$  relaxation peak shifts rapidly as the temperature changes. However, when dielectric loss is plotted against temperature, the  $\alpha$  relaxation peak can be identified clearly, as revealed in Figure 5. In contrast to the  $\beta$  relaxation peak, the  $\alpha$  peak temperature indicates less frequency dependence. This also implies that the apparent activation energy of the  $\alpha$  peak is larger than that of the  $\beta$  peak. In addition, both dielectric relaxation peaks can be observed at temperature ranges higher than those of

dynamic loss peaks because of the differences in the measuring frequencies.

Additional insight of the relaxation phenomena was obtained by the ultrasonic measurements. Although the ultrasonic spectroscopy measuring system itself can cover a wide frequency range,<sup>9</sup> the frequency range in this study was considerably narrow due to the high absorption of polyimide employed as a buffer material. According to the linear elasticity in homogeneous and isotropic solids,<sup>17</sup> the longitudinal wave velocity ( $v$ ) and attenuation ( $a$ ) are related to the complex elastic modulus ( $M$ ) with the following equations:

$$M' = \rho v^2 \quad (2)$$

$$M'' = \frac{2\rho v^3 a}{\omega} \quad (3)$$

where  $\rho$  is the density. Then, the changes in the temperature variation of the observed attenuation and velocity suggest the occurrence of mechanical relaxations. According to above equations, however, it should be noted that the peaks of the loss modulus are observed at temperatures that are a little lower than those of the wave attenuation.

As revealed in Figure 6, one can easily admit the existence of two small decreases in transmitted ultrasonic wave amplitudes, which indicate the increase of ultrasonic attenuation brought about by the  $\alpha$  and  $\beta$  relaxation processes. The key result here is the  $\beta$  relaxation peak temperature. The  $\beta$  relaxation is located as a small decrease in amplitude between 50 and 100°C. This means that the relaxation can still be observed separately from the  $\alpha$  relaxation in the MHz range. This is very different

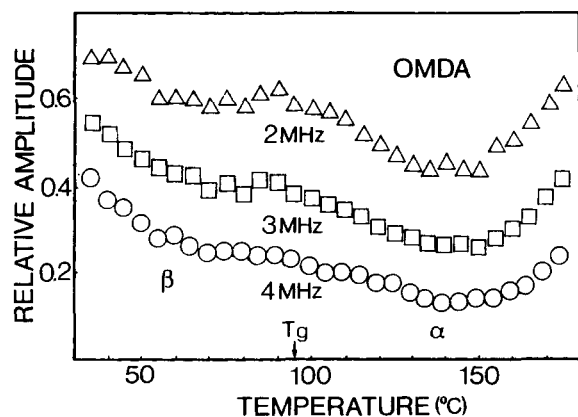


**Figure 6** Temperature dependence of ultrasonic wave amplitude in the MHz range.

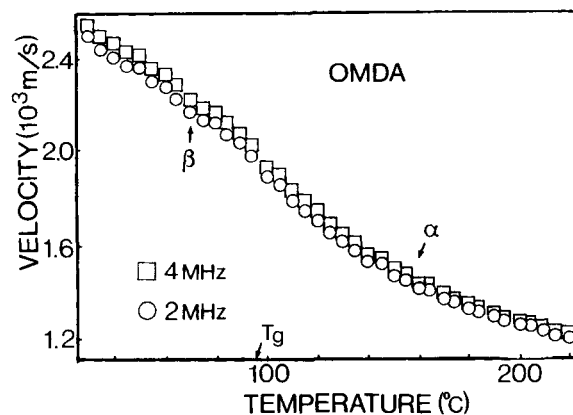


**Figure 7** Temperature dependence of ultrasonic wave velocity.

from general expectation, because at ultrasonic frequencies, most of sub  $\beta$  relaxations have been considered to overlap with the main relaxation. Figure 7 also shows the temperature variation of ultrasonic velocity at two frequencies of 2 and 4 MHz. Here, the small effect of the  $\beta$  relaxation can also be observed at temperatures below  $T_g$ . However, it should be noted that the frequency effect on the relaxation peak temperature could not be realized clearly in the observed small frequency variation.

In consideration of these results on the relaxation processes, the temperature–frequency correlation maps of the  $\alpha$  and  $\beta$  relaxation peak are derived based on the obtained data of middle-frequency dynamic, dielectric, and ultrasonic measurements. Figures 8 and 9 show the maps for the resins cured with OMDA and HMDA, respectively. The apparent activation energy can be obtained from the gradient of each relaxation map. Here, ultrasonic results are comparatively in good accordance with dynamic loss and dielectric loss data. For the  $\alpha$  relaxation peak, both of the peaks showed a similar tendency, which depends on the structure of the prepolymer used. They also exhibit an asymptotic relation to  $T_g$ , like those seen in the W.L.F.-type relaxation. Owing to the W.L.F. equation for amorphous thermoplastic polymers, the temperature–frequency correlation of the  $\alpha$  relaxation peak can be described as<sup>18</sup>

$$\text{Log} \frac{d(T)}{f_0(T_s)} = \frac{C_1(T - T_s)}{C_2 + T - T_s} \quad (4)$$

where  $T$  is the absolute temperature and  $T_s$  is reference temperature that is between  $T_g$  and 100 K above  $T_g$ .  $f$  is the frequency. In the calculation,  $T_g + 50^\circ\text{C}$  was adopted as  $T_s$ , as pointed out by Enns

and Gillham in their study of the curing process in other epoxides.<sup>19</sup> C1 and C2 are parameters, which have been reported as 8.86 and 101.6, respectively. The observed data of both sample resins are in good agreement with values calculated from this equation and show small changes of apparent activation energy.

In addition, the  $\beta$  relaxation peak changes linearly with an Arrhenius-type behavior. From this, apparent activation energies of about 16 kcal/mol are calculated for both samples. The similarity in the values of apparent activation energy also supports the model that the  $\beta$  relaxation results from a particular motion within the cross links, considering the similar structure in these resins. Moreover, molecular motions, which are considered to form the distribution of the  $\beta$  relaxation time, seem to have the same temperature–frequency correlation of relaxation peaks. From this, the  $\beta$  relaxation peak at room temperature is expected to be in the 10–100 kHz range. Taking into account the elastic wave propagation in the impact test specimen, this result does not neglect the contribution of the  $\beta$  relaxation process to the impact strength.

## CONCLUSION

We have conducted middle-frequency dynamic, dielectric, and ultrasonic measurements to investigate the main  $\alpha$  and sub  $\beta$  relaxation processes of bis-

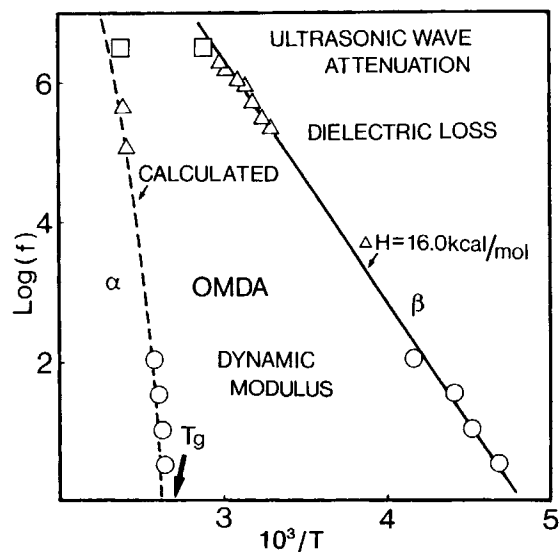


**Figure 8** Frequency–temperature correlation map of relaxation peaks obtained for the epoxides cured with OMDA.

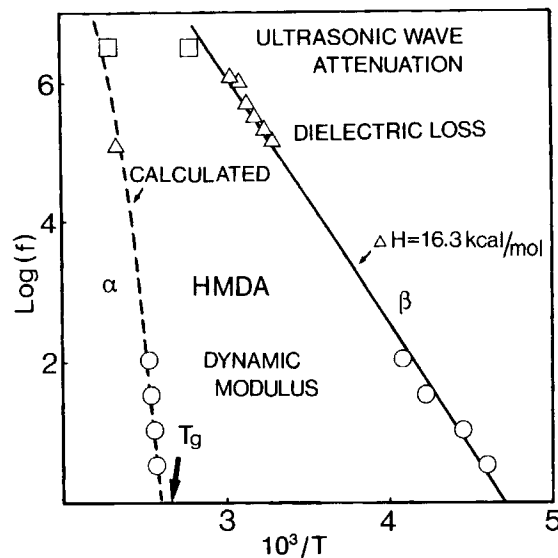


**Figure 9** Frequency–temperature correlation map of relaxation peaks obtained for the epoxides cured with HMDA.

phenol A-based epoxides cured with two different aliphatic diamines. The relaxation peaks observed by ultrasonic methods were in good accordance with other results and suggested the frequency–temperature dependence of each relaxation process. For the  $\alpha$  relaxation process, the peak temperature at lower frequencies was restricted by the glass transition temperature of the resins. It also showed the W.L.F.-type relaxation, which can be predicted as well as that for thermoplastics. For the  $\beta$  relaxation process, the peaks showed Arrhenius-type behavior, separated from the  $\alpha$  relaxation in the MHz range. They also suggest the possibility of distribution of relaxation times.

## REFERENCES

1. T. Kamon, *J. Adhes. Soc. Jpn.*, **20**, 354 (1984).
2. M. Matsukawa, Y. Tanaka, and I. Nagai, *J. Acoust. Soc. Jpn. (E)*, **13**, 2 (1992).
3. J. Mijovic and C. H. Lee, *J. Appl. Polym. Sci.*, **37**, 889 (1989).
4. Y. Wada, *J. Phys. Soc. Jpn.*, **14**, 1064 (1959).
5. R. G. C. Arridge and J. H. Speak, *Polymer*, **13**, 450 (1972).
6. G. A. Pogany, *Polymer*, **11**, 66 (1970).
7. M. Ochi, H. Iesako, S. Nakajima, and M. Shimbo, *J. Polym. Sci. Polym. Phys. Ed.*, **24**, 251 (1986).
8. M. Matsukawa, Y. Tanaka, and T. Tanaka, *Jpn. J. Appl. Phys.*, **31** (Suppl. 24-1), 26 (1992).
9. K. Matsushige, H. Okabe, S. Shichijo, and T. Take-

- mura, *Jpn. J. Appl. Phys.*, **24**(Suppl. 24-1), 34 (1985).
10. N. Hiramatsu, S. Taki, and K. Matsushige, *Jpn. J. Appl. Phys.*, **26**(Suppl. 26-1), 76 (1987).
11. W. Sachse and Y. Pao, *J. Appl. Phys.*, **49**, 4320 (1978).
12. L. E. Nielsen, *Mechanical Properties of Polymers and Composites*, Marcel Dekker, New York, 1975.
13. M. Ochi, M. Okazaki, and M. Shimbo, *J. Polym. Sci. Polym. Phys. Ed.*, **20**, 689 (1982).
14. M. B. M. Mangion and G. P. Johari, *J. Polym. Sci. Polym. Phys. Ed.*, **28**, 71 (1990).
15. N. G. McCrum, B. E. Read, and G. Williams, *Anelastic and Dielectric Effects in Polymeric Solids*, Wiley, New York, 1967.
16. T. Koike, *J. Appl. Polym. Sci.*, **44**, 679 (1992).
17. S. Timoschenko and J. N. Goodier, *Theory of Elasticity*, McGraw-Hill, New York, 1954.
18. M. L. Williams, R. F. Landel, and J. D. Ferry, *J. Am. Chem. Sci.*, **77**, 3701 (1955).
19. J. B. Enns and J. K. Gillham, *J. Appl. Polym. Sci.*, **28**, 2567 (1983).

Received July 13, 1992

Accepted January 29, 1993